

MODELING AND OPTIMIZATION OF SLIDING SPECIFIC WEAR AND COEFFICIENT OF FRICTION OF ALUMINUM BASED RED MUD METAL MATRIX COMPOSITE USING TAGUCHI METHOD AND RESPONSE SURFACE METHODOLOGY

S. Rajesh*, S. Rajakarunakaran, R. Sudhakara Pandian

Department of Mechanical Engineering, Kalasalingam University

Anand Nagar, Krishnankoil, 626 190, India

*e-mail: prindirajaki@yahoo.co.in

Abstract. Metal matrix composites (MMCs) are attracting considerable interest worldwide because of their superior mechanical and tribological properties. This investigation presents the use of Taguchi method for minimizing the specific wear and coefficient of friction in red mud based aluminum MMC. Response Surface Methodology (RSM) is also employed to develop mathematical model for specific wear rate and coefficient of friction. A plan of experiments, based on L_{27} Taguchi design method, the orthogonal array, signal- to- noise ratio, and analysis of variance (ANOVA) are employed to investigate the influence of parameters like applied load, sliding velocity, % of reinforcement and hardness of the counterpart material. Pin on Disc apparatus is used to conduct the experiment to analyze the effect of input parameters on output performance characteristics. From the analysis of signal to noise ratio (S/N) and ANOVA, the optimal combination levels and the effect of input parameter on output response are obtained. RSM is employed to develop mathematical model, capability of the model is good in prediction of results and results are very closer to the measured value. Analysis of variance (ANOVA) technique is applied to check the validity of the developed model. The result stress that the developed model could be effectively employed to predict the specific wear rate and the coefficient of friction.

1. Introduction

Aluminum metal matrix composites have been of interest as engineering materials because of their higher stiffness and specific strength, as well as superior wear resistance, compared to unreinforced aluminum alloys [1]. Superior mechanical and physical properties leads to the use of these composites in several automobile and engineering components where wear, tear and seizure are the major problems in addition to the weight saving. Some of these components are brake drums, pistons, connecting rods, cylinder heads and drive shafts for automobile sectors and impellers, agitators, turbine blade, valves, pump inlet, vortex finder for marine and mining sectors [2]. Particulate metal matrix composites (PMMCs) are of special interest owing to the low cost of their raw materials and their ease of fabrication, making them suitable for applications requiring relatively high volume production [1]. The most interesting materials commercially utilize SiC, Al_2O_3 or B_4C particles incorporated into the aluminum matrix by a variety of processes including powder metallurgy [3]. Powder metallurgy processing of aluminum MMCs first requires the combination of the aluminum

alloy powder, either as a mixture of elemental and master alloy powders or in pre alloyed form, with the reinforcement in a blending process [4]. Among the different reinforcement material, red mud emerging reinforcement because of its low cost and availability in huge quantity. Red mud emerges as the major waste material during production of alumina from bauxite by the Bayer's process [5]. The estimated annual rate of production of red mud from Bayer's process is nearly 30 million ton per year. While using a powder metallurgy technique for fabrication of MMC, best mechanical properties can be attained since reinforcement materials are homogeneously distributed over the matrix material [6]. In addition to that, in this process low temperature is used for fabrication when compared to melting process thus it avoids chemical reaction between the matrix and reinforcement material [7]. Another advantage of powder metallurgy technique is in its ability to manufacture near net shape products at low cost and give good dimensional tolerance for the complex geometries [8].

In this context, it is required to characterize red mud based aluminum composites in terms of wear under different experimental conditions. Sliding wear behavior of Aluminum Metal Matrix Composites (AMCs) has been studied by many investigators [9] however, limited attempts have been made to study the effect of red mud in aluminum matrix. It has been reported that the wear resistance of composite increases with increase in volume fraction and size of the dispersoids [10]. One of the prime factors of the improvement in wear resistance is increased in hardness of the Al-alloy due to the addition of hard dispersoids [11]. The hardness of the composite increases with increase in the volume fraction of the dispersoid but at the same time its toughness decreases [12]. The increase in volume fraction of alumina in aluminum alloy 7075 matrix increase the wear resistance of the composites [13]. It is reported that the, tribological properties of Al-Si alloy – graphite under 30-1 % relative humidity and found that the specific wear rate and coefficient of friction increased more than the base alloy material [14].

There have been few dry sliding wear behavior studies based on various reinforcements like SiC, Al₂O₃, fly ash and Zircon. The principle tribological parameters that control (load, sliding velocity, sliding distance, counterpart material, weight % of reinforcement, shape, and size) specific wear rate and coefficient of friction were analyzed [15].

From the literature it is understand that, the relationship between the parameters in dry sliding wear is complex and independent, selection of the optimal parameter of combination is important to reduce specific wear rate and coefficient of friction. Design of experiment, Genetic algorithm and response surface method is widely used to optimize the dry sliding parameters [16].

There has been experimental investigation using Taguchi and ANOVA to identify the significant factors while testing with Al 2219 SiC and Al 2219 SiC – graphite material shows that the sliding distance, sliding velocity and load are having significant effect [17]. Set of experiments conducted by a combining orthogonal arrays and ANOVA techniques to study the tribological behavior of Al-2014 alloy-10 wt.% SiC composites. It is found that the introduction of SiC particle reinforcement in the matrix alloy exerted the greatest effect on abrasive wear, followed by the applied load. The sliding distance is found to have a much lower effect [18].

It is observed that the wear resistance is strongly dependent on the sliding velocity and the hardness of the counter materials. A counter material with a lower hardness reduced the wear resistance due to the mutual abrasion between the counter material and the wear surface of the specimen [19].

Response surface method has been applied to evaluate dry sliding wear behavior of AA7075 aluminum-SiC composites produced by powder metallurgy technique, it is found that the sliding velocity is directly proportional to wear rate and the particle size and volume fraction is inversely proportional to wear rate [20]. It is inferred that the effect of load is

significant for aluminum -10% alumina composite using factorial design of experiment method. Also, the combined effect of abrasive size and sliding distance caused not only increased wear of matrix alloy but also helped to reduce the wear of composite [21].

From the above literature review, it understood that the effect of different factors and their interactions on dry sliding wear behavior of MMCs is studied extensively. However, most of the reported research works focused on the effect of either one factor or two factors on dry sliding wear behavior of MMCs. There is no systematic study has been reported so far incorporating various factors that influence the dry sliding wear behavior of MMCs. Hence, the present investigation has been carried out to optimize the wear parameters and to develop a mathematical model to predict the dry sliding wear rate of red mud based aluminum metal matrix composite material fabricated by powder metallurgy technique incorporating the effects of applied load, sliding velocity, weight % of reinforcement, and counterpart materials.

2. Methods of analysis

2.1 Response surface methodology. Response surface methodology is practical, economical and relatively easy to use. It is the combination of statistical and mathematical techniques useful for developing and optimizing the process. It is commonly applied in situations where several input potentially influence the output (response) of interest. Response methodology is generally used to explain the relationship between response factor and independent factor. For this reason, it is very important to define the response and independent factor. The selection of control factors for dry sliding wear of the composites can be attempted based on a basic understanding of the process and from the literature. A lot of factors have an effect on the specific wear rate and coefficient of friction but all of these factors could not be considered because the number of experiments would increase exponentially. Therefore, the number of independent factors is limited to four in order to reduce the number of experiments.

The first step of RSM is to define the limits of the experimental domain to be explored. These limits are made as wide as possible to obtain a clear response from the model [22]. The applied load, sliding velocity, weight % of reinforcement and different hardness counterpart material are selected variables for this investigation. In the next step is the planning to accomplish the experiments by means of RSM using the Box-Behnken method. In many engineering fields, there is a relationship between an output variable of interest (y) and a set of controllable variables (x_1, x_2, \dots, x_n). The relationship between the wear control parameters and the responses is given as:

$$y = f(x_1, x_2, \dots, x_n) + \varepsilon, \quad (1)$$

where ε represents the noise or error observed in the response (y). If we denote the expected response to be $E(y) = f(x_1, x_2, \dots, x_n) = \eta$, then the surface represented by

$$\eta = f(x_1, x_2, \dots, x_n). \quad (2)$$

Here η is called a response surface. The variables x_1, x_2, \dots, x_n in Eq. (2) are called natural variables because they are expressed in natural units of measurement.

In most RSM problems, the form of the relationship between the independent variables and the response is unknown; it is approximated. Thus, the first step in RSM is to find an appropriate approximation for the true functional relationship between response and the set of independent variables. Usually, a low-order polynomial in some region of the independent variables is employed. If the response is well modeled by a linear function of the independent variables, then the approximating function is the first order model:

$$y = \beta_0 + \beta_1 x_1 + \beta_2 x_2 + \dots + \beta_k x_k + \varepsilon. \quad (3)$$

If there is curvature in the system, then a polynomial of higher degree must be used, such as the second-order model then a polynomial of higher degree must be used, such as second order model:

$$y = \beta_0 + \sum_{j=1}^k \beta_j x_j + \sum_{j=1}^k \beta_{jj} x_j^2 + \sum_i^{k-1} \sum_j^k \beta_{ij} x_i x_j + \varepsilon, \quad (4)$$

where $i = 1, 2, \dots, k-1$ and $j = 1, 2, \dots, k$ also $i < j$ [23].

2.2 Taguchi method. A large number of experiments have to be carried out when the number of the process parameters increases. To solve this problem, the Taguchi method uses a special design of orthogonal arrays that helps to study the entire parameter space with only a small number of experiments. Taguchi's techniques consist of an experimental plan to obtain information about the behavior of a process.

Taguchi recommends analyzing the mean response for each run in the inner array, and he also suggests analyzing variation using an appropriately chosen signal-to-noise ratio (S/N). These S/N ratios are derived from the quadratic loss function and among the three, the following is "Lower – the – best" (Eq. (5)) is considered to be standard and widely applicable:

$$\frac{s}{N} = -10 \log \left(\frac{1}{n} \sum_{i=1}^n \frac{1}{y^2} \right), \quad (5)$$

where y is the average of observed data, s^2 is the variation of y , n is the number of observations [24].

The optimal setting is the parameter combination that has highest S/N ratio. The statistical analysis of the data is performed by analysis of variance (ANOVA) to study the contribution of the factor and interactions and to explore the effects of each process on the observed value [25].

3. Experimental procedure

In this work, powder metallurgy technique is used to fabricate MMC specimen, the raw material used for the study is aluminum powder with 99 % purity and average particle size in the range of 150 to 300 μm . Red mud was used as reinforcement material with composition of (Al_2O_3 - 16.8 %, SiO_2 - 15.2 %, Fe_2O_3 - 33.8 %, Na_2O_3 - 11.87 %, CaO - 2.45 %, TiO_2 - 3.7 %, Mn - 1.2 %, P_2O_5 - 0.67 % and Zn - 0.018 %) and average particle size is in the range of 1.8 to 4 μm . The density of the aluminum and red mud are 2.7 and 3.2 g/cm^3 respectively.

To fabricate MMC, red mud is preprocessed; with the help of ball mill and it is sieved to get uniform particle size of the reinforcement material. Size of the red mud particle is measured by Malvern laser size analyzer. Figure 1 shows the average particle size of the red mud reinforcement material. Figure 2 shows SEM micrograph of the red mud powder.

The required amount of aluminum and red mud particle are measured and then mixed in a planetary ball mill for 2 h under a constant speed of 150 rpm. For this purpose, four balls made of WC-Co with 80 g each are used. Ball to powder ratio 10:1 and liquid ethanol is used as a process control agent. Before green compaction process, the powder is dried in electric induction furnace at 100 °C to remove the moisture content.

Compacted specimens are obtained by pouring the required amount of powder into the die material and it is compressed uniaxially in the universal testing machine with load of 300 kN. The required number of samples has been prepared for 3, 4 and 5 % of reinforcement materials. The green compacted specimens are sintered in electric induction furnace. The sintering is done at a temperature of 600 °C and sintering time is maintained at 60 min.

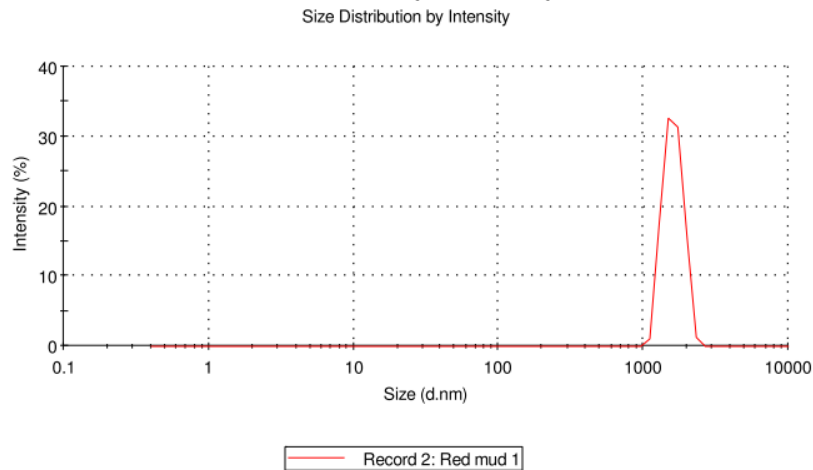


Fig. 1. Average particle of the red mud reinforcement material.

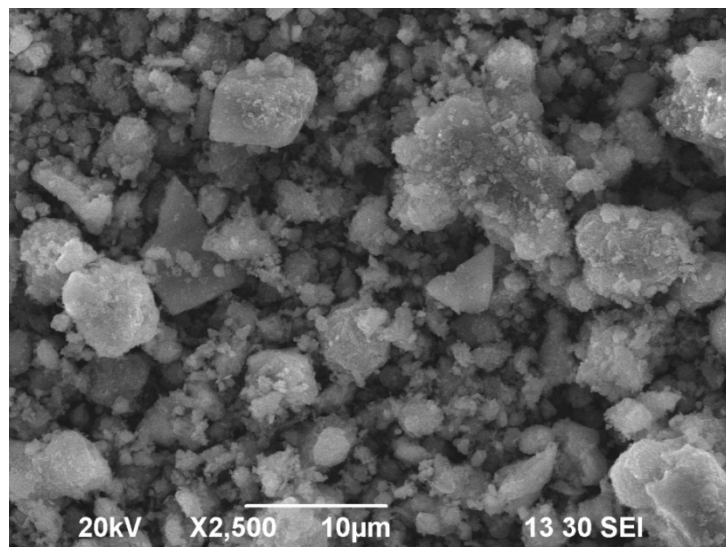


Fig. 2. SEM micrographs of red mud powder.

The distribution of reinforcement in the fabricated specimen material is examined using Scanning Electron Microscope (SEM). For micro structural characterization, the test samples are polished with different mesh number of 800 and 1000 mesh emery sheets and then the killers' reagent is used as etchant. The standard procedure is adopted to prepare the etchant using 1 volume part of hydrofluoric acid, 1.5 volume part of hydrochloric acid, 2.5 volume parts of nitric acid and 95 volume parts of water.

The fabricated specimens are subjected to test the density and hardness. The density of the base aluminum alloy and composites are determined using Archimedes's principle. The samples are precision weighted in an electronic balance (make: Shimadzu-TXC 623 L) to an accuracy of 0.0001 gm. Hardness tests are carried out on a Brinell hardness testing machine (Make: Saroj Hardness machine) using a load of 750 kg for 15 sec. Four measurements have been taken on different areas and the mean value is taken for each sample.

The pin on disc is used to evaluate the specific wear rate and coefficient of friction response to the sliding contact surface of specimens as shown in the Fig. 3. Tests are conducted under dry sliding conditions as per the ASTM G 99-95. The pin is initially cleaned with acetone and weighed accurately using a digital electronic balance. This carried out applying normal load (10, 30, and 50 N) and for constant sliding distance 3000 m at different sliding velocities (2, 3 and 4 m/s).



Fig. 3. Photograph of the pin on disc apparatus.

Totally three different hardness counterpart material is used to conduct the experiment with following specification. EN 32 with 58 and 60 hardness and alumina oxide with 62 HRC is used. At the end of the each test, the specimen is again weighed in the same balance after cleaning with acetone. The difference between the initial and final weights is a measure of slide mass loss. The mass loss is then converted into volume loss using the corresponding density values. The specific wear rate is calculated by converting volume less to sliding distance. The specific wear rate (W_s) is calculated using the following equation:

$$W_s = \frac{\Delta m}{\rho F n L}, \quad (6)$$

where W_s is the specific wear rate, Δm is the mass loss, ρ is the density, n is the normal load and L the sliding distance. After the test, the sliding surface of test samples is observed by scanning electron microscopy (SEM).

4. Design of experiments

4.1 Taguchi analysis. In this study, four parameters are selected as control factors, and each parameter is designed to have three levels, denoted 1, 2, and 3. The experimental design is according to L_{27} (3^4) array based on Taguchi method. Based on the preliminary experimentation it is decided that four independent variables namely, load, sliding velocity, weight % of reinforcement and counterpart material could influence the magnitude of dry sliding. The sliding distance is kept constant at 3000 m for all the experimental runs. The levels of these factors chosen for the study are given in Table 1.

The response variables to be studied are the specific wear rate and coefficient of friction. Experimental results of the specific wear rate and coefficient of friction with various parameters are shown in Table 2. From the experimental results, the S/N ratios for each experiment of L_{27} (3^4) is calculated by applying Eq. (5). The objective of using the S/N ratio as a performance measurement is to develop products and process insensitive to noise factor. Thus, by utilizing experiment results and computed values of the S/N ratios (Table 2), average S/N response ratio is calculated for specific wear rate and coefficient of friction. Table 3 and Figure 4 show average effect response table for specific wear.

Table 1. Independent variable and their level.

Level	Factors			
	Load, N	Sliding velocity, m/s	% of reinforcement	Counterpart material HRC
1	10	2	3	58
2	30	3	4	60
3	50	4	5	62

Table 2. Orthogonal array of Taguchi for wear and friction coefficient.

Load in N	Sliding velocity, m/sec	% of reinforcement	Disc	Specific wear rate, $\text{mm}^3/\text{N}\cdot\text{m} \times 10^{-13}$	S/N ratio	Friction coefficient	S/N ratio
10	2	3	1	3.3659	-10.5420	0.489	6.2138
10	2	4	2	6.269	-15.9440	0.365	8.7541
10	2	5	3	8.2369	-18.3153	0.276	11.1818
10	3	3	2	7.9945	-18.0558	0.578	4.7614
10	3	4	3	13.2156	-22.4217	0.385	8.2908
10	3	5	1	15.2389	-23.6591	0.356	8.9710
10	4	3	3	4.269	-12.6065	0.312	10.1169
10	4	4	1	13.567	-22.6497	0.392	8.1343
10	4	5	2	11.289	-21.0531	0.295	10.6036
30	2	3	1	1.239	-1.8614	0.631	3.9994
30	2	4	2	1.56	-3.8625	0.615	4.2225
30	2	5	3	5.5216	-14.8413	0.315	10.0338
30	3	3	2	1.1236	-1.0122	0.685	3.2862
30	3	4	3	15.259	-23.6705	0.4	7.9588
30	3	5	1	10.5698	-20.4813	0.562	5.0053
30	4	3	3	7.369	-17.3482	0.416	7.6181
30	4	4	1	8.369	-18.4535	0.525	5.5968
30	4	5	2	5.239	-14.3850	0.386	8.2683
50	2	3	1	0.1139	18.8695	0.656	3.6619
50	2	4	2	0.2149	13.3553	0.6	4.4370
50	2	5	3	10.11569	-20.0999	0.395	8.0681
50	3	3	2	0.99268	0.0638	0.615	4.2225
50	3	4	3	10.2569	-20.2203	0.462	6.7072
50	3	5	1	13.697	-22.7325	0.401	7.9371
50	4	3	3	3.269	-10.2883	0.425	7.4322
50	4	4	1	11.239	-21.0146	0.385	8.2908
50	4	5	2	5.369	-14.5979	0.351	9.0939

Regardless of category of the quality characteristic, a greater S/N ratio corresponds to a better performance. The level of a factor with the highest signal-to-noise ratio is the optimum level [26]. Therefore, the optimal parameter combination level identified for the present investigation in the process is load at level 3 (A3), sliding velocity at level 1 (B1), % of reinforcement at level 1 (C1) and disc material at level 2 (D2) for specific wear rate.

Table 3. Average experimental results and S/N response table for specific wear rate.

Level	A	B	C	D
1	-18.361	-5.916	-5.865	-13.614
2	-12.880	-16.910	-14.987	-8.388
3	-8.518	-16.933	-18.907	-17.757
Delta	9.842	11.017	13.043	9.369
Rank	3	2	1	4

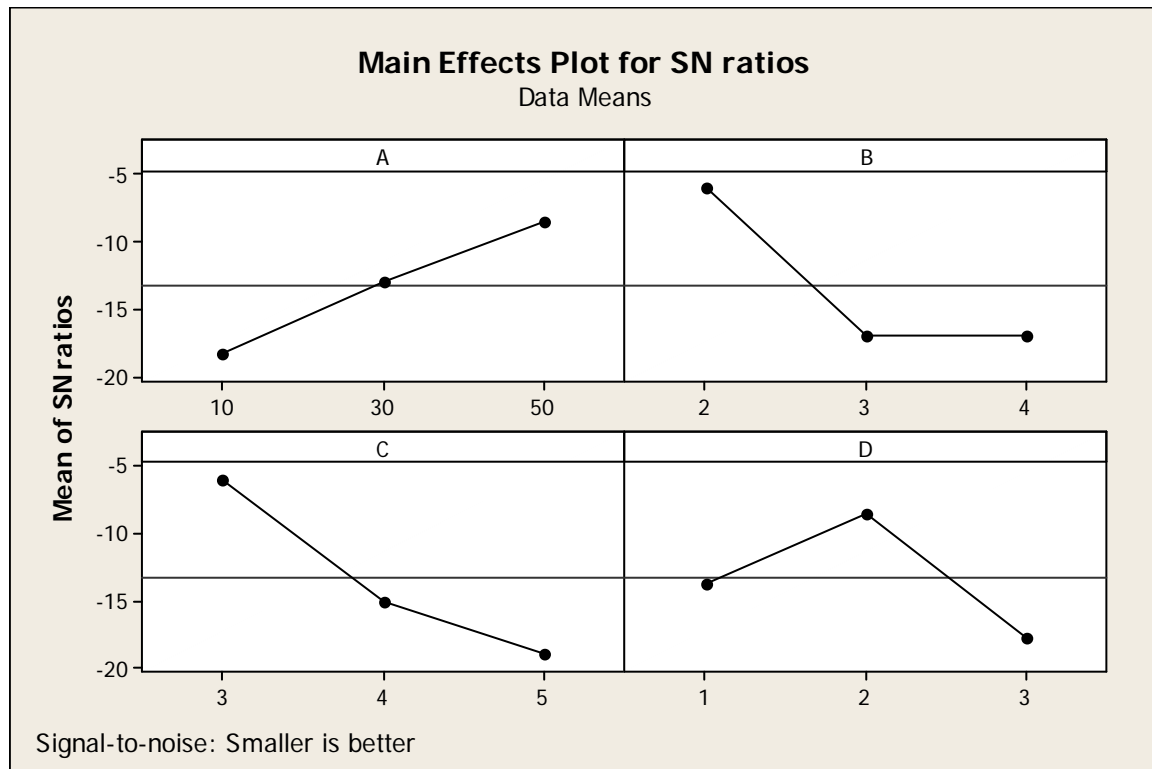


Fig. 4. Effect of wear parameters on specific wear rate.

Based on the results of the S/N ratio and experimental, the optimal parameters for specific wear rate are obtained at 50 N applied load (level 3), 2 m/s sliding velocity (level 1), 3 % of reinforcement (level 1) and 60 HRC counterpart material level (2).

From Table 4 and Fig. 5, the optimum conditions for the coefficient of friction can be established. Based on the results of the S/N ratio and experimental results, the optimal parameters for coefficient of friction is obtained at 10 N applied load (level 1), 4 m/s sliding velocity (level 3), 5 % of reinforcement (level 3) and counterpart material (level 3).

The purpose of the statistical ANOVA is to investigate which design parameter significantly affects the specific wear rate and coefficient of friction. Tables 5 and 6 show the results of the ANOVA analysis for the specific wear and coefficient of friction respectively. This analysis is carried out for a significance level of $\alpha = 0.05$, i.e., for confidence level of 95 %. Tables 5 and 6 show that the probability levels are the realized significance levels, associated with the F tests for each source of variation. The sources with a probability level less than 0.05 are considered to have a statistically significant contribution to the performance measures. Also, last columns of Tables 5 and 6 show the percentage of contribution of each source to the total variation, indicating the degree of influence on the result. From Table 5 it is

understand that the specific wear rate of the aluminum based red mud MMC are applied load L (10.8 %), sliding velocity (29.2 %), % of reinforcements (39.9 %) and counterpart material (19.86 %). From the analysis of Table 6, it is inferred that the significant factor for coefficient of friction are MMC applied load L (21.4 %), sliding velocity (18.2 %), % of reinforcements (35.6 %) and counterpart material (24.7 %).

Table 4. Average experimental results and S/N response table for coefficient of friction.

Level	A	B	C	D
1	8.559	6.73	5.701	6.423
2	6.221	6.349	6.932	6.405
3	6.650	8.351	8.796	8.601
Delta	2.338	2.002	3.094	2.195
Rank	2	4	1	3

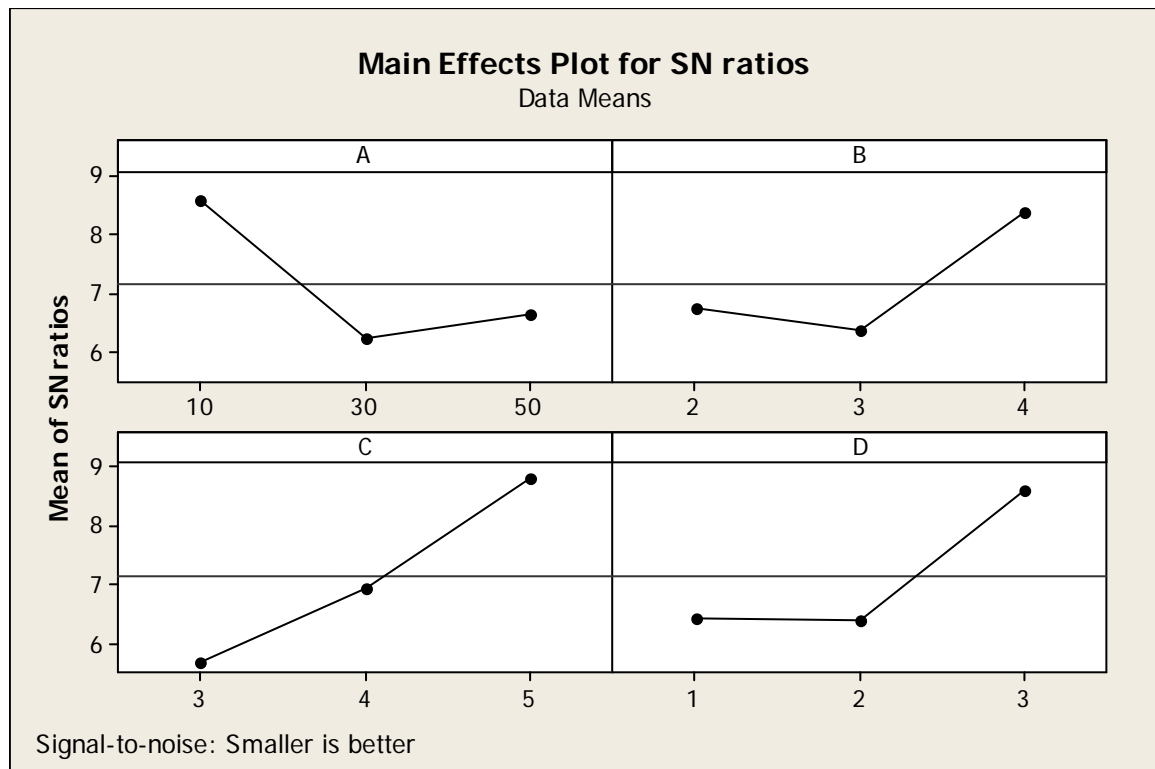


Fig. 5. Effect of wear parameters on coefficient of friction.

Table 5. ANOVA for specific wear rate.

Source	DF	Seq SS	Adj SS	Seq MS	F	P	% of contribution
A	2	56.836	56.836	28.418	6.13	0.009	10.8
B	2	152.709	152.709	76.355	16.48	0.000	29.2
C	2	208.686	208.686	104.343	22.52	0.000	39.9
D	2	103.637	103.637	51.819	11.18	0.001	19.86
Error	18	83.392	83.392	4.633			
Total	26	26	605.260				

R-Sq = 86.22 %, R-Sq(adj) = 80.10 %

Table 6. ANOVA for Coefficient of friction.

Source	DF	Seq SS	Adj SS	Adj MS	F	P	% of contribution
A	2	0.072243	0.072243	0.036121	13.31	0.000	21.4
B	2	0.061381	0.061381	0.030690	11.31	0.001	18.2
C	2	0.120291	0.120291	0.060145	22.16	0.000	35.6
D	2	0.083318	0.083318	0.041659	15.35	0.000	19.86
Error	18	0.048846	0.048846	0.002714			
Total	26	0.386079					

R-Sq = 87.35 %, R-Sq(adj) = 81.72 %

4.2 Correlation of optimum results with surface morphology of specimen. The optimized result can be correlated with SEM micrographs of the worn surface red mud based aluminum MMC composites.

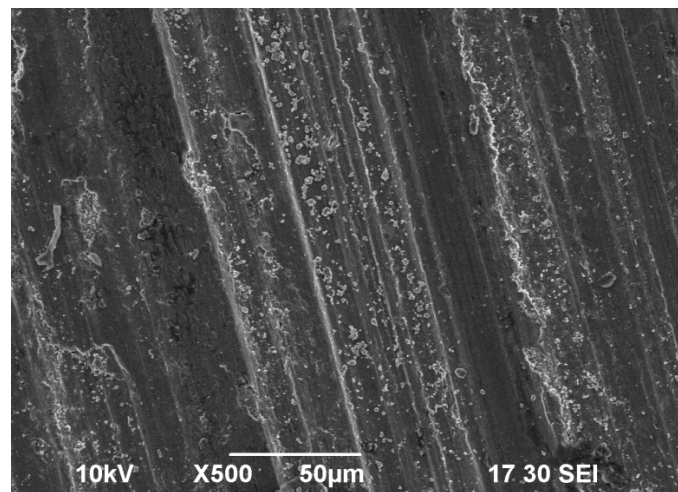


Fig. 6. Wear surface of 3 % of red mud reinforcement under the load of 50 N, sliding velocity 2 m/s and counterpart hardness 60 HRC.

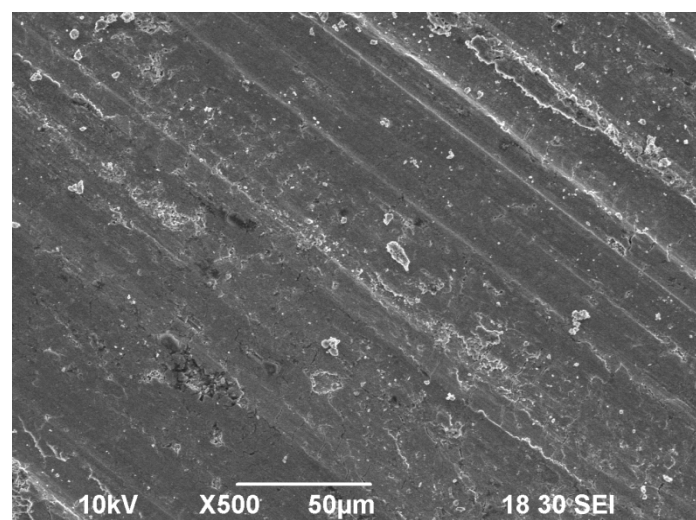


Fig. 7. Wear surface of 3 % of red mud reinforcement under the load of 50 N, sliding velocity 4 m/s and counterpart hardness 62 HRC.

Figure 6 SEM image shows the wear surface of the red mud based aluminum MMC tested at applied load 50 N, sliding velocity 2 m/s, 3 % of reinforcement and counterpart material hardness is 60 HRC. This micrograph shows numerous long grooves; fewer deformation and craters on wear surfaces. Figure 7 shows the wear surface of the red mud based aluminum MMC tested at applied load 50 N, sliding velocity 4 m/s, 3 % of reinforcement and counterpart material hardness is 62 HRC, leads to more particle pullout.

4.3 Response Surface analysis. In analyzing the specific wear rate and coefficient of friction in wear tests, statistical models play an important role. These models are used for prediction of results. RSM's design consisting of 29 experiments is calculated for developing the mathematical model for specific wear rate and coefficient of friction. Tables 7 and 8 give the model summary statistics for specific wear rate and coefficient of friction, respectively. These tables reveal that quadratic model is the best suggested model for specific wear rate and coefficient of friction. So, for further analysis, this model is used.

Table 7. Model summary for specific wear rate.

Source	Std. Dev.	R-Squared	Adjusted R-Squared	Predicted R-Squared	PRESS	
Linear	3.215196	0.459131	0.368986	0.181142	375.6145	
2FI	3.417907	0.541584	0.286909	-0.39139	638.2368	
Quadratic	2.336927	0.83332	0.666639	0.093969	415.601	Suggested
Cubic	1.860095	0.954743	0.7888	-3.68297	2148.101	Aliased

Table 8. Model Summary for coefficient of friction.

Source	Std. Dev.	R-Squared	Adjusted R-Squared	Predicted R-Squared	PRESS	
Linear	0.161883	0.430711	0.33583	0.114771	0.977993	
2FI	0.115067	0.784279	0.664433	0.315003	0.756779	
Quadratic	0.085009	0.908425	0.816851	0.530311	0.518908	Suggested
Cubic	0.100246	0.945423	0.745308	-4.89834	6.516436	Aliased

The relative importance of the dry sliding parameters with respect to the specific wear rate and coefficient of friction is investigated to determine more accurately the optimum combinations of the wear parameters using ANOVA. Table 9 gives the ANOVA results for the response surface quadratic model for specific wear rate. The values of "Prob > F" in Table 9 for the model <0.1000 indicates that model terms are significant. In this case A, B, C, D, C² and D² are significant model terms. Other model terms can be said to be not significant. These insignificant model terms can be removed and may result in an improved model.

From Table 9, the model F value of 4.99 indicates that the model is still significant. The values of Prob > F <0.1000 show that model terms are important. The R² (0.83) value is high, close to 1, which is desirable. The predicted R² (0.72) is in reasonable agreement with the adjusted R². Adequate precision measures the S/N ratio. A ratio greater than 4 indicates adequate model discrimination. In this particular case, it is 10.39, which indicates an adequate signal. It is noted that interaction among wear parameters is insignificant, while the independent effects of dry sliding wear parameters are also significant. Therefore, applied load (A), sliding velocity (B), weight % of reinforcement (C), counterpart material (D) C² and D² are significant terms.

Table 9. ANOVA for Specific wear rate.

Source	Sum of squares	df	Mean square	F value	p-value Prob > F	
Model	382.2481	14	27.30343	4.999506	0.0024	significant
A-applied load	76.95356	1	76.95356	14.09089	0.0021	
B-sliding velocity	58.18124	1	58.18124	10.65351	0.0057	
C-% of reinforcement	49.22451	1	49.22451	9.013455	0.0095	
D-Hardness of the material	26.24633	1	26.24633	4.805942	0.0458	
AB	1.0201	1	1.0201	0.18679	0.6722	
AC	0.375892	1	0.375892	0.068829	0.7969	
AD	7.3441	1	7.3441	1.344771	0.2656	
BC	7.7841	1	7.7841	1.425339	0.2524	
BD	7.570752	1	7.570752	1.386273	0.2587	
CD	13.72703	1	13.72703	2.513543	0.1352	
A ²	0.059107	1	0.059107	0.010823	0.9186	
B ²	5.223644	1	5.223644	0.956497	0.3447	
C ²	102.3209	1	102.3209	18.73588	0.0007	
D ²	19.83895	1	19.83895	3.632693	0.0774	
Residual	76.45716	14	5.461226			
Lack of Fit	70.55072	10	7.055072	4.77788	0.0726	not significant
Pure Error	5.906445	4	1.476611			

Table 10 ANOVA for coefficient of friction.

Source	Sum of squares	df	Mean square	F value	p-value Prob > F	
Model	1.00362	14	0.071687	9.920065	< 0.0001	significant
A-applied load	0.108376	1	0.108376	14.99707	0.0017	
B-Sliding velocity	0.1728	1	0.1728	23.91205	0.0002	
C-% of reinforcement	0.11167	1	0.11167	15.45286	0.0015	
D-Hardness of the material	0.083	1	0.083	11.48558	0.0044	
AB	0.0121	1	0.0121	1.674397	0.2166	
AC	0.047437	1	0.047437	6.564307	0.0226	
AD	0.116281	1	0.116281	16.09096	0.0013	
BC	0.0196	1	0.0196	2.712247	0.1218	
BD	0.1936	1	0.1936	26.79036	0.0001	
CD	0.0016	1	0.0016	0.221408	0.6452	
A ²	0.016195	1	0.016195	2.241008	0.1566	
B ²	0.001512	1	0.001512	0.209205	0.6544	
C ²	0.075355	1	0.075355	10.42764	0.0061	
D ²	0.018232	1	0.018232	2.522943	0.1345	
Residual	0.101171	14	0.007226			
Lack of Fit	0.085963	10	0.008596	2.260987	0.2243	not significant
Pure Error	0.015208	4	0.003802			

Table 10 gives the ANOVA for the response surface quadratic model for coefficient of friction. From Table 10, the model F value of 9.92 implies that the model is significant for coefficient of friction. The value of “Prob > F” for model is < 0.1000, which indicates, that the model terms are significant. In this case A, B, C, D, AC, AD, BD and C² are significant model terms. There is only 0.01 % chance that a “model F value” this large could occur due to noise. The R² (0.85) value is high, close to 1, which is desirable. The predicted R² (0.79) is in reasonable agreement with the adjusted R². Adequate precision measures the S/N ratio. A ratio greater than 4 indicates adequate model discrimination. In this particular case, it is 15.35, which indicates an adequate signal. Therefore, the model can be used to navigate the design space.

The mathematical relationship for correlating output response to input parameters is calculated by Design Expert software version 8.01. The following equations are the final empirical model in terms of coded factors for specific wear rate (Y1) and coefficient of friction (Y2).

$$\text{Specific wear rate} = 3.093 - 2.53 A - 2.2 B + 2.03 C - 1.48 D + 1.35 AD - 1.39 BC + 1.85 CD - 0.91 B^2 + 3.95 C^2 + 1.73 D^2, \quad (7)$$

$$\text{Coefficient of friction} = 0.497 - 0.095 A + 0.12 B - 0.09 C - 0.05 D - 0.11 AC + 0.17 AD + 0.22 BD + 0.04 A^2 - 0.11 C^2 + 0.05 D^2. \quad (8)$$

The normal probability plots of the residuals versus the predicted response for specific wear rate and coefficient of friction are shown in Figs. 8 and 9 respectively.

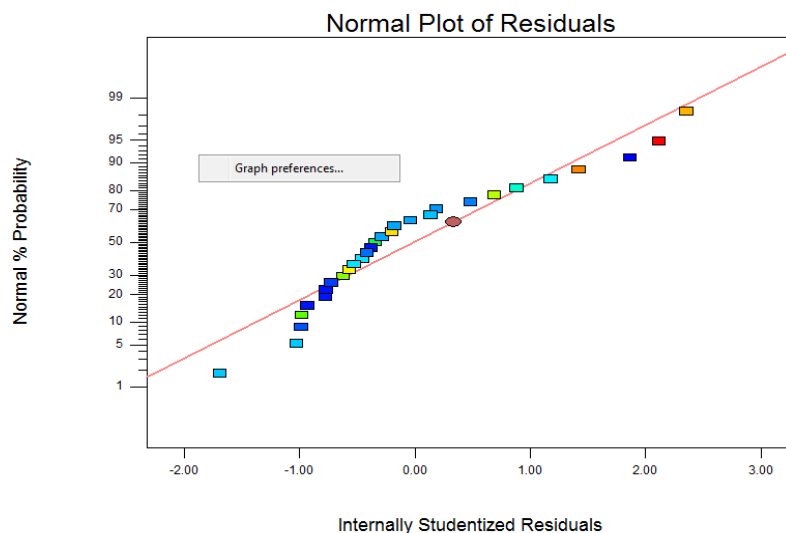


Fig. 8. Residual plot for specific wear rate.

Figures 8 and 9 revealed that the residuals generally fall on a straight line, implying that the errors are normally distributed. This implies that the models proposed are adequate, and there is no reason to suspect any violation of the independence or constant variance assumption [27].

From the developed RSM-based mathematical model, the effect of parameter on specific wear rate is examined. Figures 10, 11, and 12 show 3D graphs of specific wear rate as a function of dry sliding wear parameters.

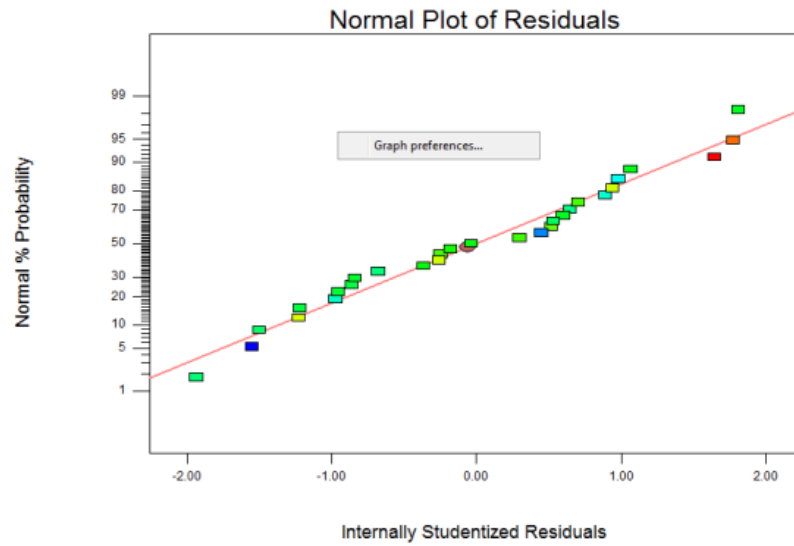


Fig. 9. Residual plot for coefficient of friction.

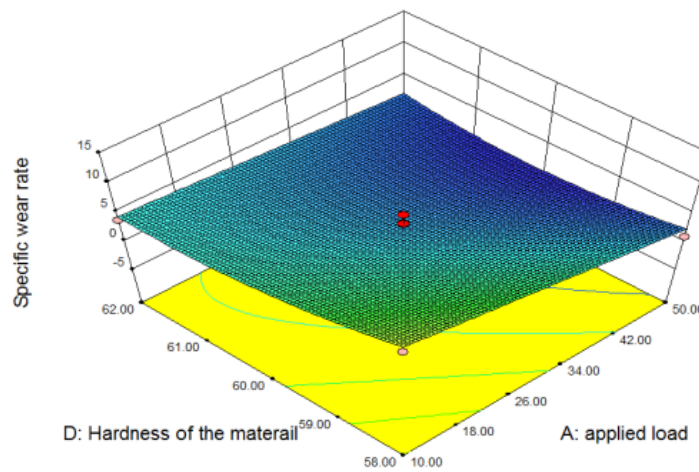


Fig. 10. 3D surface graph of specific wear rate as function of applied load and hardness of the counterpart material.

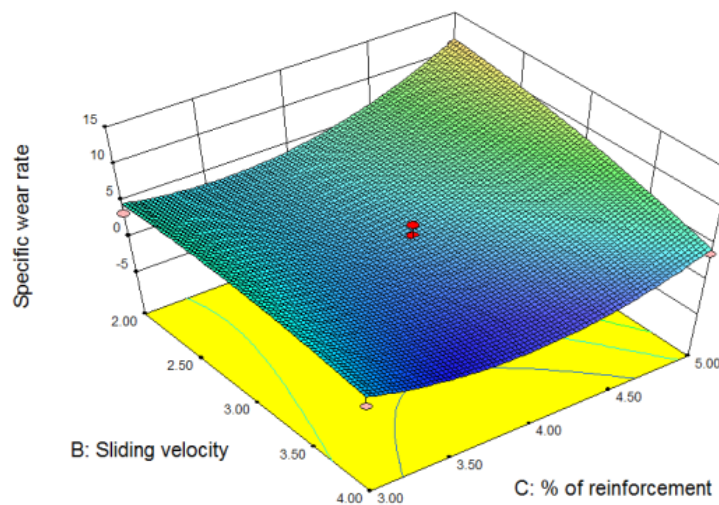


Fig. 11. 3D surface graph of specific wear rate as function of sliding velocity and weight % of reinforcement.

From Fig. 10, it is observed that specific wear rate of the composites increases while increasing the applied load and hardness of the counterpart material at constant sliding velocity and weight % reinforcement. From Fig 11, it is understand that specific wear rate of the composites increases with increasing sliding velocity and % of reinforcement while keeping applied load and counterpart material at constant values. From Fig 12, it is inferred that specific wear rate increase while increasing the hardness of the material and sliding velocity. From Figs.13 and 14, the lowest coefficient of friction is obtained at lowest sliding velocity and hardness of the counterpart material. From Fig. 15, the coefficient of friction increases with increases in applied load and weight % of reinforcement.

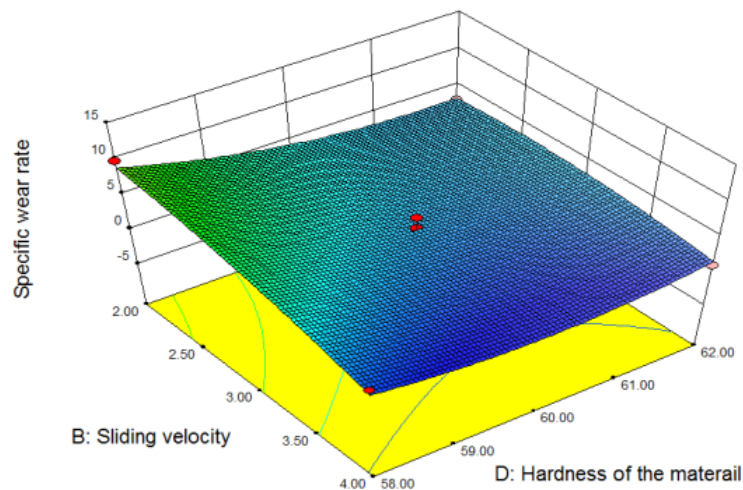


Fig. 12. 3D surface graph of specific wear rate as function of sliding velocity and hardness of the counterpart material.

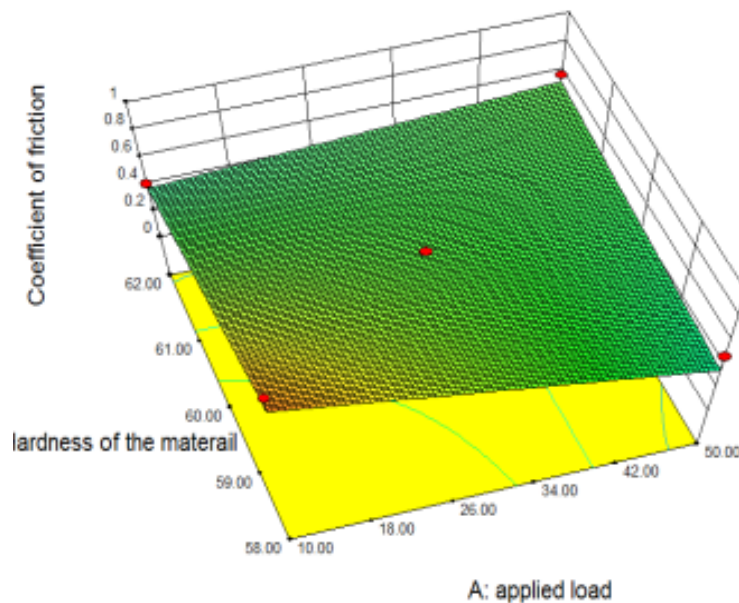


Fig. 13. 3D surface graph of coefficient of friction as function of applied load and hardness of the counterpart material.

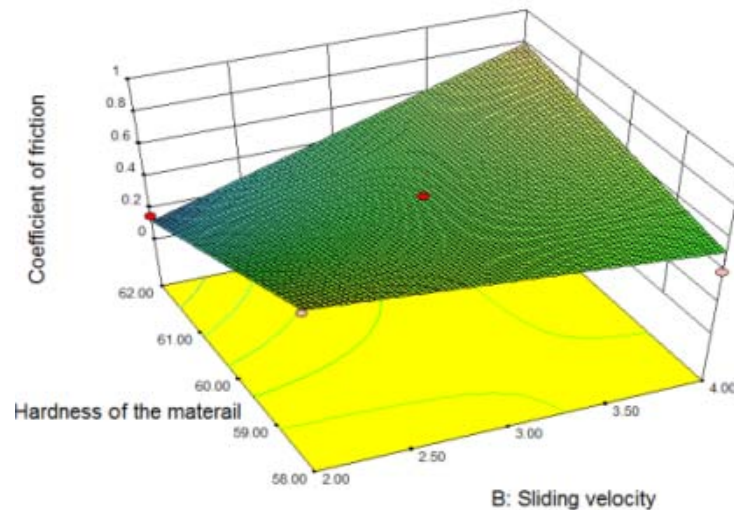


Fig. 14. 3D surface graph of coefficient of friction as function of sliding velocity and hardness of the counterpart material.

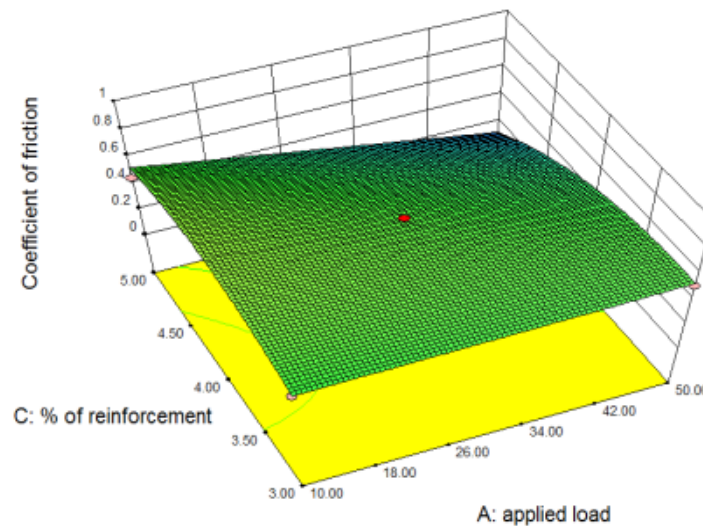


Fig. 15. 3D surface graph of coefficient of friction as function of applied load and weight % of reinforcement.

5. Conclusions

This paper has presented an application of Taguchi method and response surface methodology for selecting the optimum combination values and mathematical model of dry sliding wear parameters affecting the specific wear rate and coefficient of friction in red mud based aluminum composites fabricated through powder metallurgy technique. The conclusions of this present study are drawn as follows:

Taguchi method has been found as the most successful technique to perform trend analysis of the specific wear rate and the coefficient of friction with respect to various combinations of dry sliding wear parameters. S/N ratio is used to identify the optimal combination dry sliding wear parameters. The lowest specific wear occurs at high load, low sliding velocity, low % of reinforcement and medium level counterpart material hardness. The optimal level for the specific wear rate is A₃, B₁, C₁ and D₂. The optimal level for coefficient of friction is A₁, B₃, C₃ and D₃. The results of ANOVA reveal that % of reinforcement is the main dry sliding parameters, which has greater influence on the specific wear rate and coefficient of friction.

RSM has been used to develop mathematical model for specific wear rate and coefficient of friction for various dry sliding wear parameters. The quadratic models developed using RSM are reasonably accurate and can be used for prediction within the limits of the factors investigated. From RSM model and experiment results, the predicted and measured values are quite close, which indicates that the developed model can be effectively used to predict the specific wear rate and the coefficient of friction.

Reference

- [1] B.G. Park, A.G. Crosky, A.K. Hellier // *Composites: Part B* **39** (2008) 1257.
- [2] S. Das, D.P. Mondal, O.P. Modi, R. Dasgupta // *Wear* **231** (1999) 195.
- [3] Naiqin Zhao, Philip Nash, Xianjin Yang // *Journal of Materials Processing Technology* **170** (2005) 586.
- [4] G.T. Campbell, R. Raman, R. Fields, In: *Powder Metallurgy Aluminum and Light Alloys for Automotive Applications*, ed. by W.F. Jandeska Jr., R.A. Chernenkoff (Metal Powder Industries Federation, Princeton, NJ, 1998), p. 43.
- [5] Acharya SK, Mishra P. // *Journal of Reinforced Plastics and Composites* **27** (2008), 145.
- [6] Hossein Abdizadeh, Maziar Ashuri, Pooyan Tavakoli Moghadam, Arshia Nouribahadory, Hamid Reza Baharvandi // *Materials & Design* **32** (2011) 4417.
- [7] A.R. Nesarikar, S.N. Tewari, E.E. Graham // *Materials Science and Engineering* **147** (1991) 191.
- [8] Mehdi Rahimian, Nader Parvin, Naser Ehsani // *Materials & Design* **32** (2011) 1031.
- [9] G. Straffelini, F. Bonollo, A. Molinari, A. Tiziani // *Wear* **221** (1997) 192.
- [10] S. Sawla, S. Das // *Wear* **257** (2004) 555.
- [11] Lee Huei-Long, Lu Wun-Hwa, Sammy Lap-Ip Chan // *Wear* **159** (1992) 223.
- [12] Kassim S Al-Rubaie, Humberto N Yoshimura, José Daniel Biasoli de Mello // *Wear* **233–235** (1999) 444.
- [13] A. Daoud, T. El-Bitar, A. Abd El-Azim // *Journal of Materials Engineering and Performance* **12** (2003) 390.
- [14] B.K. Yen, T. Ishihara // *Wear* **198** (1996) 169.
- [15] A.P. Sannino, H.J. Rack // *Wear* **189** (1995) 1.
- [16] S. Dharmalingam, R. Subramanian, K. Somasundara Vinoth, B. Anandavel // *Journal of Materials Engineering and Performance* **20** (2010) 1457.
- [17] S. Basavarajappa, G. Chandramohan, J. Paulo Davim // *Materials & Design* **28** (2007) 1393.
- [18] Y. Sahin // *Materials & Design* **28** (2007) 1348.
- [19] H. Turhan, O. Yilmaz // *Zeitschrift für Metallkunde* **93** (6) (2002) 572.
- [20] S. Kumar, V. Balasubramanian // *Wear* **264** (2008) 1026.
- [21] O.P. Modi, R.P. Yadav, D.P. Monal, R. Dasgupta, S. Das, A.H. Yegneswaran // *Journal of Materials Science* **36** (2001) 1601.
- [22] M.K. Pradhan, C.K. Biswas, In: *Proceedings of NCMSTA'08 Conference* (Hamirpur, 2008), p. 535.
- [23] R.H. Myers, D.C. Montgomery, *Response surface methodology: process and product optimization using designed experiment* (Wiley, New York, 1995).
- [24] N.S. Mohan, S.M. Kulkarni, A. Ramachandra // *J. Mater. Process Technol.* **186** (2007) 265.
- [25] D.C. Montgomery, *Design and analysis of experiments* (Arizona State University, New York, 1991).
- [26] W.H. Yang, Y.S. Tarn // *Journal of Material Process Technology* **84** (1998) 122.
- [27] K. Palanikumar // *International Journal of Advanced Manufacturing Technology* **36** (2008) 19.